



Published in final edited form as:

*Langmuir*. 2009 May 19; 25(10): 5725–5730. doi:10.1021/la803963r.

## Dynamic Seeding of Perfusing Human Umbilical Vein Endothelial Cells (HUVECs) onto Dual-Function Cell Adhesion Ligands: Arg-Gly-Asp (RGD)-Streptavidin and Biotinylated Fibronectin

Charles C. Anamelechi<sup>†</sup>, Edward C. Clermont<sup>‡</sup>, Matthew T. Novak<sup>†</sup>, and William M. Reichert<sup>\*,†</sup>

<sup>†</sup>Biomedical Engineering Department, Duke University, 136 Hudson Hall, Durham, North Carolina 27708

<sup>‡</sup>School of Medicine, Emory University, 1648 Pierce Drive, Atlanta, Georgia 30322

### Abstract

Surfaces decorated with high affinity ligands can be used to facilitate rapid attachment of endothelial cells; however, standard equilibrium cell detachment studies are poorly suited for assessing these initial adhesion events. Here, a dynamic seeding and cell retention method was used to examine the initial attachment of perfusing human umbilical vein endothelial cells (HUVECs) to bare Teflon-AF substrates, substrates pre-adsorbed with fibronectin alone, or substrates co-pre-adsorbed with two dual-function cell-adhesion ligands: biotinylated fibronectin (bFN) and RGD-streptavidin mutant (RGD-SA). Cell attachment was evaluated as a function of cell trypsinization (integrin digestion), surface protein formulation, and cell perfusion rate. Surfaces co-pre-adsorbed with bFN and RGD-SA showed the highest density of attached cells after 8 min of perfusion and the highest percent retention when subjected to shear flow at 60 dynes/cm<sup>2</sup> for 2 min. Surfaces with no ligand treatment showed the lowest cell attachment and retention under flow in all cases. HUVECs trypsinized with mild 0.025% trypsin/ethylenediaminetetraacetic acid (EDTA) showed greater cell adhesion after perfusion and higher percent retention after shear flow than those trypsinized using harsher 0.05% trypsin/EDTA. The preferential affinities of the two dual-function ligands for  $\alpha_5\beta_1$  and  $\alpha_v\beta_3$  integrins were also examined by surface plasmon resonance (SPR) spectroscopy. The dynamic cell seeding studies confirmed that the dual-function ligand system promotes HUVEC adhesion and retention at short time points when tested using a perfusion assay. SPR studies showed that the two ligands exhibited equal affinity for both  $\alpha_5\beta_1$  and  $\alpha_v\beta_3$  integrins but that the combined ligands bound more total integrins than the two ligands tested separately.

## Introduction

The interaction between endothelial cells (ECs) and extracellular matrix (ECM) components play a central role in regulating cell morphology, growth, differentiation, and motility.<sup>1-4</sup> These effects have broader implications on adhesion and attachment of ECs to biomaterials, such as synthetic vascular grafts.<sup>5,6</sup> The adhesion-promoting ECM proteins fibronectin (FN), laminin (LN), and vitronectin (VN) are multidomain molecules that interact mainly with cell-surface integrin receptors.<sup>7-9</sup> The most widely studied ECM cell-binding domain, the tripeptide Arg-Gly-Asp (RGD), preferentially binds to specific transmembrane integrins based on location and orientation.<sup>10,11</sup> Moreover, positioning and density of the RGD-binding motifs on the polymer materials play an important role on focal adhesion (FA) formation and cell migration.<sup>1,12</sup>

Binding of ECs to surfaces pre-adsorbed with cell adhesion proteins is dominated by two main integrins:  $\alpha_5\beta_1$  and  $\alpha_v\beta_3$ . Once ECs bind, integrins cluster to induce complexation of proteins on the cytoplasmic side of the membrane,<sup>13</sup> which in turn initiates early actin polymerization.<sup>14</sup> These “early-stage” focal contacts are rich in  $\alpha_v\beta_3$  integrins. In the presence of FN,  $\alpha_5\beta_1$  integrins modulate the formation of fibrillar adhesions, while  $\alpha_v\beta_3$  promotes the development of mature focal contacts.<sup>15,16</sup> Specific interactions of FN with  $\alpha_5\beta_1$  are augmented by the PHSRN synergy site, while  $\alpha_v\beta_3$  mediated interactions are not affected synergistically. These two integrin-dependent pathways have been shown to independently activate actin polymerization and maturation of matrix adhesions to mature focal contacts.

The formation of the first few bonds during initial cell-substrate contact is a critical step in the cell adhesion process.<sup>17</sup> To augment these initial cell adhesion events, we developed a system of dual-function ligands bFN and RGD-SA.<sup>18-20</sup> Previous application of the dual-function ligands to human umbilical vein endothelial cell (HUVEC) adhesion on Teflon-AF polymer substrates involved the decoration of cells with mutant strain RGD-SA, followed by statically seeding the cells onto substrates pre-adsorbed with bFN. Surprisingly, dual-function ligand-treated HUVECs did not exhibit significantly enhanced spreading or retention when tested with this static cell retention methodology.<sup>20</sup> It thus became apparent that either the dual-function ligands were being deployed ineffectively and/or the use of static (e.g., equilibrium) cell adhesion methodologies were incapable of detecting differences in initial cell adhesion events. To address these limitations, we made two major changes to the experimental protocol.

First, rather than using static cell-seeding methods, the surfaces were perfused with cells and the dynamic attachment of cells to the surfaces was measured. Extensive work has been conducted with similar perfusion systems to examine monocyte tethering and rolling to approximate adhesion to vascular endothelium,<sup>21</sup> characterize platelet adhesion,<sup>22</sup> and measure the affects of shear stress on monocyte rolling and adhesion.<sup>23</sup> Researchers have also used dynamic seeding to measure hepatocytes binding onto polymer constructs<sup>24,25</sup> and to quantify flowing platelet adhesion on surfaces pre-adsorbed with exogenous proteins.<sup>26</sup> Kim et al. also combined dynamic seeding with static culture to produce skin tissue using fibroblasts,<sup>27</sup> and Burg et al. combined a dynamic seeding system with a bioreactor

proliferation phase to increase cellular adhesion and proliferation for three-dimensional polymer scaffolds.<sup>28</sup> To date, similar efforts using ECs in a flow perfusion system have not been tried.

Second, rather than decorating cells with RGD-SA before seeding them on the bFN-treated substrate, we sequentially co-pre-adsorbed substrates with bFN and then RGD-SA, followed by perfusing the surface with unmodified HUVECs. This eliminated the rearrangement or internalization of the RGD-SA mutant by cells incubated with the ligand. The co-pre-adsorbed dual-function ligands take advantage of the density of RGD-binding motifs introduced using highly specific streptavidin-biotin binding to preferentially augment the binding of the two dominant transmembrane integrins  $\alpha_5\beta_1$  and  $\alpha_v\beta_3$ .

In brief, the dynamic cell attachment studies confirmed the utility of the dual-function ligands in achieving increased initial cell attachment after 8 min of perfusion, as well as increasing the percent cell retention when subjected to a short burst of laminar flow, with the most mildly trypsinized HUVEC showing higher percent retention after flow. The preferential affinities of the two dual-function ligands for  $\alpha_5\beta_1$  and  $\alpha_v\beta_3$  integrins were also demonstrated by surface plasmon resonance (SPR) spectroscopy. These studies thus establish an experimental framework for studying the early events of endothelial cell adhesion onto surfaces modified with exogenous cell-binding proteins.

## Materials and Methods

### Dual-Function Cell-Adhesion Ligands

RGD-SA mutant protein and bFN were prepared and characterized as previously reported.<sup>20,29</sup> RGD-SA mutant was constructed using the technique of cassette mutagenesis, in which a 60-mer oligonucleotide was annealed into the synthetic SA gene. This process introduced an RGD motif into each monomer of SA. Biotinylated fibronectin was produced with 100 M excess sulfo-NHS-LC-biotin (Pierce, Rockford, IL), with a spacer arm of 2.2 nm. The bFN was coupled with an average of nine biotins per FN molecule as determined using EZ-Link-NHS-chromogenic-biotin (Pierce), with a polyethylene glycol spacer arm of 4.1 nm and a bis-aryl hydrazone group with a characteristic absorbance at 354 nm. Absorbance values were indicative of the number of biotins per fibronectin.

### Cell Culture

All cell-culture reagents were obtained from Cambrex (Walkersville, MD), unless specified otherwise. HUVECs were grown to confluence in gelatin-coated T25 poly-styrene flasks (Corning, Inc., Corning, NY) with endothelial basal media (EBM) supplemented with 0.5 mL of 10 mg/mL human recombinant epidermal growth factor (hEGF), 0.5 mL of 1.0 mg/mL hydrocortisone, 0.5 mL of 50 mg/mL gentamicin, 50 mg/mL amphotericin-B mix, 3 mg/mL bovine brain extract (BBE), and 10 mL of fetal bovine serum (FBS). Cells were cultured in an incubator with 95% air/5% CO<sub>2</sub> at 37 °C. Two confluent T-25 HUVECs from passage 3–6 were rinsed with dPBS without Ca<sup>2+</sup> and Mg<sup>2+</sup>, incubated with 2 mL each of either 0.025 or 0.05% trypsin/ethylenediaminetetraacetic acid (EDTA) for 4 min at 37 °C, neutralized with trypsin-neutralizing solution (TNS), and centrifuged at 2200 rpm for 5 min.

For all experiments,  $1 \times 10^6$  cells were diluted into 8 mL of fresh serum-free media, treated with 64  $\mu\text{L}$  of Hoechst dye 33342 (Molecular Probes, Carlsbad, CA), rotated in an incubator for 15 min, then transferred to a 10 mL syringe prior to use in the cell infusion assembly.

### Static Cell-Seeding Experiments

Static cell retention analysis was performed as previously published<sup>30</sup>, with minor modifications. Briefly, HUVECs were treated with Hoechst dye (Molecular Probes), placed in an incubator for 40 min, and then seeded for 15 min onto Teflon-AF-coated glass slides pre-adsorbed with 20  $\mu\text{g}/\text{mL}$  bFN, rinsed with dPBS with  $\text{Ca}^{2+}$  and  $\text{Mg}^{2+}$ , and then incubated with 7 mL of 50  $\mu\text{g}/\text{mL}$  of RGD-SA for 40 min at room temperature. The slides were assembled into a laminar flow chamber. A total of 20 images were obtained preflow at marked points on the flow chamber using a fluorescence microscope. At this point, a flow loop was assembled, and the cells were exposed to flow at a shear stress of 60 dynes/cm<sup>2</sup> for 2 min using dPBS with  $\text{Ca}^{2+}$  and  $\text{Mg}^{2+}$ . Postflow images obtained at the same points along the chamber were used to measure relative percent retention. Surfaces with no protein pretreatment served as controls. Images were analyzed in Image J using a macro written in Matlab.

### Dynamic Cell-Seeding Experiments

Teflon-AF-coated slides were incubated with Dulbecco's phosphate-buffered saline (dPBS) with  $\text{Ca}^{2+}$  and  $\text{Mg}^{2+}$  for 1 h in a quadriperm plate for the "no ligand" surface and treated with 20  $\mu\text{g}/\text{mL}$  of FN or bFN solution for 1 h in the "FN alone" and "bFN alone" cases and then rinsed with dPBS with  $\text{Ca}^{2+}$  and  $\text{Mg}^{2+}$  prior to assembling into the flow chamber. For the other two experimental formulations, Teflon-AF slides were incubated with 20  $\mu\text{g}/\text{mL}$  bFN for 1 h in the quadriperm plate, rinsed with dPBS with  $\text{Ca}^{2+}$  and  $\text{Mg}^{2+}$ , and then incubated with 7 mL of 50  $\mu\text{g}/\text{mL}$  of RGD-SA or WT-SA for 40 min at room temperature. After the incubation period, slides were rinsed, assembled into a laminar flow chamber, and used in a flow infusion loop. With this system, we examined cell attachment and retention because of protein surface modification, trypsin/EDTA isolation method, and infusing flow rate.

The dynamic seeding system consisted of a 10 mL syringe mounted on a Harvard Apparatus pump, infusing cells onto Teflon-AF slides contained in a flow chamber over a microscope stage. During infusion, 30 s movies were captured on the different treatments to quantify the number of cells bound in real time and to analyze the behavior of cells to determine rolling (data not shown). After infusion at 1 mL/min, slides were rinsed at 2.5 mL/min for 1 min to remove unattached cells remaining in the chamber. After rinse, preflow images were taken at 20 marked imaging sites on the flow chamber. These figures were used to determine the total number of cells attached. The cells were then detached at a shear stress of 60 dynes/cm<sup>2</sup> for 2 min. After shear stress perturbation, postflow images were obtained at the same sites and used to determine cell retention values. Images were analyzed in Image J using a macro written in Matlab.

## SPR Studies

The SPR procedure was described in details elsewhere.<sup>20</sup> Briefly, cleaned glass slides were evaporated with a 4 nm adhesion promoting layer of chromium and then 20 nm of gold under vacuum to yield transparent gold films. Gold-coated slides were stored under argon until used.<sup>20,31</sup> Self-assembled monolayers (SAMs) were formed on the gold surface by immersion in solution of 2 mM 16-mercaptohexadecanoic acid (HDA) in 100% ethanol for 24 h. Afterward, chips were rinsed and dried under N<sub>2</sub> gas.

The SPR experiments were performed on a BIACOREX (Pharmacia Biosensor) microfluidic system. After chip insertion, the surface with HDA SAM was activated by injection of 35  $\mu$ L of an equal mix of 0.1 M *N*-hydroxysuccinimide (NHS) and 0.4 M 1-ethyl-3-(3-(dimethyl-amino)propyl)carbodiimide (EDC) in PBS, at a flow rate of 5  $\mu$ L/min. After flushing and baseline equilibration, 20  $\mu$ g/mL bFN, 50  $\mu$ g/mL RGD-SA, or bFN plus RGD-SA was immobilized onto the chip surface at a flow rate of 2  $\mu$ L/min. Subsequently, soluble  $\alpha_5\beta_1$  and  $\alpha_v\beta_3$  integrins (Chemicon, Billerica, MA), purified from human smooth muscle cells and verified for binding in a RGD manner dependent upon FN-coated surfaces, were flowed over the protein at 2  $\mu$ L/min. Response units (RUs) were measured on the basis of differences in the refractive index. These units were converted to protein surface density, where 1000 RU = 1 ng/mm<sup>2</sup> protein. The binding kinetics and amount bound to the surface were calculated with BIAevaluation software (Biacore AB, Uppsala, Sweden).

## Statistical Analysis

StatView 5.0 was used to statistically compare data and measure variability. One-way analysis of variation (ANOVA) plus Tukey-Kramer post hoc analyses were conducted to determine *p* values. All data were reported as the mean  $\pm$  standard error (SE).

## Results

Five ligand surface treatments were examined: no ligand, Fn alone, bFN alone, bFN + RGD-SA, and bFN + WT-SA. The wild-type SA strain (WT-SA) was included to mask the effect of the RDG ligand. Perfusing HUVECs diluted in 8 mL in serum-free media were dynamically seeded onto all surfaces, and attachment and percent retention were determined after shearing at 60 dynes/cm<sup>2</sup> for 2 min. Given recent observations of the importance of cell trypsinization methods,<sup>32</sup> we also compared cells isolated using 0.025% trypsin/EDTA and 0.05% trypsin/EDTA on all surfaces. Lastly, seeding and retention at various infusion rates were compared on DL surfaces. In general, we observed that cells adhered abruptly with little evidence of cell rolling, even on the no ligand surfaces.

## Static Cell-Seeding Experiments

Figure 1 shows percent cell retention of unmodified HUVECs seeded statically onto Teflon-AF surfaces with different protein formulations. These cells used the mild trypsinization method. Percent retention ranged from a low of 40% for no ligand surfaces to a high of 93% on bFN + RGD-SA surfaces, while FN alone and bFN + RDG-SA were statistically higher than cell retention on no ligand and bFN + WT-SA surfaces (*p* < 0.05). While this difference was expected, the cell retention on bFN + RGD-SA was of the same order as the FN alone

(86%) and bFN alone (81%) surfaces and was statistically indistinguishable from bFN + WT-SA.

### Dynamic Cell-Seeding Experiments

Figure 2A shows the number of cells that attached during 8 min of perfusion at 1 mL/min with mildly trypsinized HUVEC (0.025% trypsin/ EDTA). Many cells near the surface attached upon contact, while those flowing in lamella away from the surface merely streaked by without surface contact. The number of adherent cells ranged from  $1.1 \times 10^5$  cells on slides with the no ligand treatment to  $2.8 \times 10^5$  cells on slides with bFN + RGD-SA, with FN, bFN, and bFN + RGD-SA surfaces all having more than twice as many cells attached compared to the surface with no ligand. Figure 2B shows the percent of initially adherent mildly trypsinized HUVEC that were retained after exposure to 60 dynes/cm<sup>2</sup> laminar flow for 2 min. Percent retention ranged from a low of 19% for no ligand surfaces to a high of 89% on bFN + RGD-SA surfaces. For all surfaces, the order of cell retention was bFN + RGD-SA > FN alone > bFN alone > bFN + WT-SA > no ligand. The number and percent retention of mildly trypsinized HUVEC on the bFN + RGD-SA were significantly higher compared to all other groups ( $p < 0.05$ ). The number and percent retention of mildly trypsinized HUVEC on FN alone and bFN alone surfaces were statistically indistinguishable.

Figure 3A shows the analogous cell attachment and cell retention data for HUVECs treated with harsher trypsinization (0.05% trypsin/EDTA). The number of adherent cells ranged from a low of  $1.8 \times 10^4$  cells on the slide with no ligand treatment to a high of  $1.7 \times 10^5$  cells on the slides with bFN + RGD-SA, representing 6- and 1.6-fold reductions, respectively, in cell attachment compared to mildly trypsinized cells. Figure 3B shows the percent retention of harshly trypsinized HUVEC after exposure to 60 dynes/cm<sup>2</sup> laminar flow. Again, the order of cell retention was bFN + RGD-SA > FN alone > bFN alone > bFN + WT-SA > no ligand. Cell retention ranged from a low of 2% for no ligand surfaces to a high of 47% on bFN + RGD-SA surfaces, which were 9.5- and 1.8-fold decreases, respectively, compared to mildly trypsinized cells. The number and percent retention of harshly trypsinized HUVECs on the bFN + RGD-SA surfaces were not statistically higher relative to any surface except the no ligand case ( $p < 0.05$ ). Again, the number and percent retention of harshly trypsinized HUVECs on FN alone and bFN alone surfaces were statistically indistinguishable.

A final consideration with the dynamic seeding system was the effect of the HUVEC perfusion rate on cell attachment and retention. Figure 4A shows a steady decrease in the number of mildly trypsinized HUVEC attached as a function of the perfusion flow rate (harshly trypsinized cells were not tested). The number of adhered cells after 8 min of perfusion decreased steadily from  $2.8 \times 10^5$  at 1 mL/min to 750 at 80 mL/min. Figure 4B shows a similar downward trend of the cell retention data with an increasing perfusion flow rate.

## SPR Analysis

SPR analysis on FN alone, bFN, RGD-SA, and bFN + RGD-SA treated surfaces was performed to determine if  $\alpha_v\beta_3$  or  $\alpha_5\beta_1$  integrins showed any preferential binding. Figure 5 shows results for integrin binding to immobilized proteins. In general, FN alone, bFN, and RGD-SA surfaces bound nearly equivalent amounts of total integrins,  $3.6 \times 10^{12}$ ,  $3.4 \times 10^{12}$ , and  $3.9 \times 10^{12}$  molecules/mm<sup>2</sup>, respectively; however, FN and bFN surfaces showed a preference for  $\alpha_5\beta_1$ , while RGD-SA surfaces showed a preference for  $\alpha_v\beta_3$ . In contrast, the bFN + RGD-SA surfaces showed no affinity preference for either integrin and also bound nearly 25% more total integrins,  $4.3 \times 10^{12}$  molecules/mm<sup>2</sup>, than the FN and bFN surfaces.

## Discussion

*In vitro* characterization of EC seeded onto immobilized ECM proteins commonly uses static cell-seeding methods to assess the degree of adhesion,<sup>33–35</sup> but this approach has had limited success in assessing initial cell adhesion events. The current study examined cell adhesion and retention of HUVECs dynamically seeded onto Teflon-AF surfaces as a function of the protein treatment, trypsinization method, and perfusion flow rate. A previously developed system of dual-function ligands was modified to increase the experimental efficiency to *in vivo* applications and availability of surface integrins for binding by eliminating the direct incubation of RGD-SA with the cells prior to incubation.<sup>18,20,36</sup>

The primary goal of the current study was to show that increasing the intrinsic and extrinsic density of RGD moieties on the surface leads to greater initial cell attachment and retention of HUVEC. A dynamic seeding system was used to demonstrate that the dual-function ligands bFN + RGD-SA surface treatment promoted significantly higher initial HUVEC attachment and retention that was not evident by conventional static seeding methods. The dual-function ligands had the greatest effect on HUVEC trypsinized with mild 0.025% trypsin/EDTA, showing statistically higher adhesion and retention compared to all other tested surface treatments. Cells trypsinized with harsher 0.05% trypsin/EDTA showed the same trend as the mild trypsin treatment but at markedly decreased cell adhesion and cell retention after flow.

Of note was that perfusing cells, regardless of trypsinization protocol, attached and were retained at higher levels with the dual-function ligands compared to other protein surface treatments, but this difference was substantially lower for harshly trypsinized cells. This drop in cell adhesion and retention has been attributed in previous studies to damage of transmembrane integrins under harsh digestion of the cell membrane proteins at the higher trypsin/EDTA level.<sup>32</sup> These results suggest that the dual-function ligands bound cells with greater affinity to accessible integrins, but this effect was reduced by harsher trypsinization. Mild trypsinization reduced transmembrane integrin damage and thus retained the integrity of transmembrane integrins that interact with the presented RGD moieties on the Teflon-AF surface. The ability of RGD to bind multiple integrins would aid cells to bind, remodel, and form focal adhesions.<sup>37,38</sup>

SPR studies showed that binding of  $\alpha_5\beta_1$  and  $\alpha_v\beta_3$  integrins to surfaces immobilized with either FN alone, bFN, or RGD-SA were virtually mirror images of each other; however, when immobilized in tandem, the dual-function ligands bound nearly 25% more total bound integrin than bFN or RGD-SA separately. These results demonstrate the ability of the dual-function ligand system to bind these two integrins, possibly exhibiting a degree of cooperativity beyond a simple summing effect.

Others have reported phenomenological differences in cell retention through distinct integrin pathways.<sup>12,15</sup> While  $\alpha_5\beta_1$  appears to dominate on surfaces with either whole fibronectin or FNIII<sub>10</sub> with FNIII<sub>9</sub>, there is a decrease in the activation of focal adhesion kinase (FAK) necessary for mature focal contacts on these surfaces when using  $\alpha_v\beta_3$  integrins.<sup>10,39</sup> These observations highlight the preferential binding for specific integrins by RGD cell-binding motifs with and without the synergy site. The higher binding of  $\alpha_5\beta_1$  on surfaces with bFN alone is indicative of the need for the synergy site to facilitate this rapid interaction. Conversely, surfaces with RGD-SA alone bound  $\alpha_v\beta_3$  more abundantly and preferentially over  $\alpha_5\beta_1$  integrins. These results indicate that  $\alpha_v\beta_3$  integrins bind more preferentially to RGDs without any synergy site needed, and this dominates over  $\alpha_5\beta_1$ .<sup>40</sup> We postulate that the dual-function ligands present a surface with RGD motifs in proximity to the fibronectin synergy site PHSRN while also providing RGD motifs on the RGD-SA that are more efficiently bound by  $\alpha_v\beta_3$  integrins.

Dynamic seeding of ECs prior to static culture in the 4 mm polyurethane resulted in 90% cell coverage and retention over a period of 3–7 days.<sup>41</sup> The system presented in the current study shows close to 30% of injected ECs attached after 8 min of perfusion, and close to 90% of these cells were retained after a burst of 60 dynes/cm<sup>2</sup> shear flow without static culture. While static culture allows seeded cells to equilibrate with the surface, the ability to bind flowing EC using the protein system described here would be an advantage in promoting *in situ* cell immobilization. Rotational seeding systems currently in use<sup>41,43,44</sup> have been successful in creating endothelialized vessels *in vitro*. The main challenge with rotational systems is that the time required for desired cell attachment and coverage ranged from 7 to 10 days, while cells attached using the dual-function ligand system demonstrated actin polymerization after 1 h of attachment, indicative of a phenotypic shift toward forming mature focal contacts.<sup>20</sup> Our dual-function ligand system can be adapted to use proven seeding technologies to attach autologous cells onto synthetic vessels prior to implantation.

## Conclusions

A system of dual-function ligands was used to increase RGD density on Teflon-AF, leading to enhanced initial cell attachment under dynamic cell seeding, as well as greater percent retention compared to all other surface treatments examined. There was a substantial overall reduction in cell adhesion and retention when harsher trypsinization conditions were used, but the dual-function ligands still outperformed all other surfaces tested. SPR analysis confirmed that both of the dual-function ligands separately bound  $\alpha_5\beta_1$  and  $\alpha_v\beta_3$  integrins with different preferences, whereas surfaces co-pre-adsorbed with both ligands showed no integrin preference and bound 25% more integrin overall. The current studies demonstrate the ability of this approach to rapidly bind and tether endothelial cells in a perfusion system



by using integrin-mediated binding. These observations may have utility with immobilizing flowing ECs to promote cell adhesion and endothelialization at short time points.

## References

1. Cavalcanti-Adam EA, Volberg T, Micoulet A, Kessler H, Geiger B, Spatz JP. *Biophys J*. 2007; 92(8):2964–2974. [PubMed: 17277192]
2. Hynd MR, Frampton JP, Dowell-Mesfin N, Turner JN, Shain W. *J Neurosci Methods*. 2007; 162(1–2):255–263. [PubMed: 17368788]
3. Howe A, Aplin AE, Alahari SK, Juliano RL. *Curr Opin Cell Biol*. 1998; 10(2):220–231. [PubMed: 9561846]
4. Garcia AJ, Vega MD, Boettiger D. *Mol Biol Cell*. 1999; 10(3):785–798. [PubMed: 10069818]
5. Prendiville EJ, Coleman JE, Callow AD, Gould KE, Laliberte-Verdon S, Ramberg K, Connolly RJ. *Eur J Vasc Surg*. 1991; 5(3):311–319. [PubMed: 1864396]
6. Schneider A, Schwalb H, Vlodavsky I, Uretzky G. *Clin Mater*. 1993; 13 (1–4):51–55. [PubMed: 10146243]
7. Preissner KT. *Annu Rev Cell Biol*. 1991; 7:275–310. [PubMed: 1725600]
8. Massia SP, Rao SS, Hubbell JA. *J Biol Chem*. 1993; 268(11):8053–8059. [PubMed: 8463322]
9. Honduvilla NG, Bujan J, Lizarbe MA, Bellon JM, Olmo N, Hernando A. *Artif Organs*. 1991; 2:144–153.
10. Petrie TA, Capadona JR, Reyes CD, Garcia AJ. *Biomaterials*. 2006; 27(31):5459–5470. [PubMed: 16846640]
11. Keselowsky BG, Collard DM, Garcia AJ. *Proc Natl Acad Sci US A*. 2005; 102(17):5953–5957.
12. Massia SP, Hubbell JA. *J Cell Biol*. 1991; 114(5):1089–1100. [PubMed: 1714913]
13. Coussen F, Choquet D, Sheetz MP, Erickson HP. *J Cell Sci*. 2002; 115(part 12):2581–2590. [PubMed: 12045228]
14. Miyamoto S, Akiyama SK, Yamada KM. *Science*. 1995; 267(5199):883–885. [PubMed: 7846531]
15. Zamir E, Geiger B. *J Cell Sci*. 2001; 114:3583–3590. [PubMed: 11707510]
16. Zamir E, Katz M, Posen Y, Erez N, Yamada KM, Katz BZ, Lin S, Lin DC, Bershadsky A, Kam Z, Geiger B. *Nat Cell Biol*. 2000; 2(4):191–196. [PubMed: 10783236]
17. Tissot O, Pierres A, Foa C, Delaage M, Bongrand P. *Biophys J*. 1992; 61(1):204–215. [PubMed: 1540690]
18. Bhat VD, Truskey GA, Reichert WM. *J Biomed Mater Res*. 1998; 40(1):57–65. [PubMed: 9511099]
19. Chan BP, Chilkoti A, Reichert WM, Truskey GA. *Biomaterials*. 2003; 24(4):559–570. [PubMed: 12437950]
20. Anamelechi CC, Clermont EE, Brown MA, Truskey GA, Reichert WM. *Langmuir*. 2007; 23(25):12583–12588. [PubMed: 17985940]
21. Rinker KD, Prabhakar V, Truskey GA. *Biophys J*. 2001; 80(4):1722–1732. [PubMed: 11259286]
22. Gerszten RE, Lim YC, Ding HT, Snapp K, Kansas G, Dichek DA, Cabanas C, Sanchez-Madrid F, Gimbrone MA Jr, Rosenzweig A, Lusinskas FW. *Circ Res*. 1998; 82(8):871–878. [PubMed: 9580553]
23. Pritchard WF, Davies PF, Derafshi Z, Polacek DC, Tsao R, Dull RO, Jones SA, Giddens DP. *J Biomech*. 1995; 28(12):1459–1469. [PubMed: 8666586]
24. Kim SS, Sundback CA, Kaihara S, Benvenuto MS, Kim BS, Mooney DJ, Vacanti JP. *Tissue Eng*. 2000; 6(1):39–44. [PubMed: 10941199]
25. Shvartsman I, Dvir T, Harel-Adar T, Cohen S. *Tissue Eng, Part A*. 2008; 14(00):1–10. [PubMed: 18333800]
26. Feuerstein IA, McClung WG, Horbett TA. *J Biomed Mater Res*. 1992; 26(2):221–237. [PubMed: 1569115]
27. Xiao YL, Riesle J, Blitterswijk CAV. *J Mater Sci: Mater Med*. 1999; 10(12):773–777. [PubMed: 15347949]

28. Burg KJ, Holder WD Jr, Culberson CR, Beiler RJ, Greene KG, Loeb sack AB, Roland WD, Eiselt P, Mooney DJ, Halberstadt CR. *J Biomed Mater Res*. 2000; 51(4):642–649. [PubMed: 10880112]
29. McDevitt TC, Nelson KE, Stayton PS. *Biotechnol Prog*. 1999; 15(3):391–396. [PubMed: 10356256]
30. Anamelechi CC, Truskey GA, Reichert WM. *Biomaterials*. 2005; 26 (34):6887–6896. [PubMed: 15990164]
31. Smith JT, Tomfohr JK, Wells MC, Beebe TP Jr, Kepler TB, Reichert WM. *Langmuir*. 2004; 19:8279–8286. [PubMed: 15350103]
32. Brown MA, Wallace CS, Anamelechi CC, Clermont E, Reichert WM, Truskey GA. *Biomaterials*. 2007; 28(27):3928–3935. [PubMed: 17570483]
33. Weatherford DA, Sackman JE, Reddick TT, Freeman MB, Stevens SL, Goldman MH. *Surgery*. 1996; 120(2):433–439. [PubMed: 8751615]
34. Becquemin JP, Riff Y, Kovarsky S, Ardaillou N, Benhaien-Sigaux N. *J Cardiovasc Surg*. 1997; 38(1):7–14. [PubMed: 9128115]
35. Shimada T, Nishibe T, Miura H, Hazama K, Kato H, Kudo F, Murashita T, Okuda Y. *Surg Today*. 2004; 34(12):1025–1030. [PubMed: 15580386]
36. Chan BP, Reichert WM, Truskey GA. *Biotechnol Prog*. 2004; 2:566–575. [PubMed: 15059004]
37. Hersel U, Dahmen C, Kessler H, Hersel U, Dahmen C, Kessler H. *Biomaterials*. 2003; 24(24): 4385–4415. [PubMed: 12922151]
38. Massia SP, Hubbell JA. *J Biomed Mater Res*. 1991; 25(2):223–242. [PubMed: 1829082]
39. Hocking DC, Sottile J, McKeown-Longo PJ. *J Cell Biol*. 1998; 141 (1):241–253. [PubMed: 9531562]
40. Ochsenhirt SE, Kokkoli E, McCarthy JB, Tirrell M. *Biomaterials*. 2006; 27(20):3863–3874. [PubMed: 16563498]
41. Hsu SH, Tsai IJ, Lin DJ, Chen DC. *Med Eng Phys*. 2005; 27(3):267–272. [PubMed: 15694611]
42. Bordenave L, Fernandez P, Remy-Zolghadri M, Villars S, Daculsi R, Midy D. *Clin Hemorheol Microcirc*. 2005; 33(3):227–234. [PubMed: 16215288]
43. Soletti L, Nieponice A, Guan J, Stankus JJ, Wagner WR, Vorp DA. *Biomaterials*. 2006; 27(28): 4863–4870. [PubMed: 16765436]
44. Nasser BA, Pomerantseva I, Kaazempur-Mofrad MR, Sutherland FW, Perry T, Ochoa E, Thompson CA, Mayer JE Jr, Oesterle SN, Vacanti JP. *Tissue Eng*. 2003; 9(2):291–299. [PubMed: 12740091]

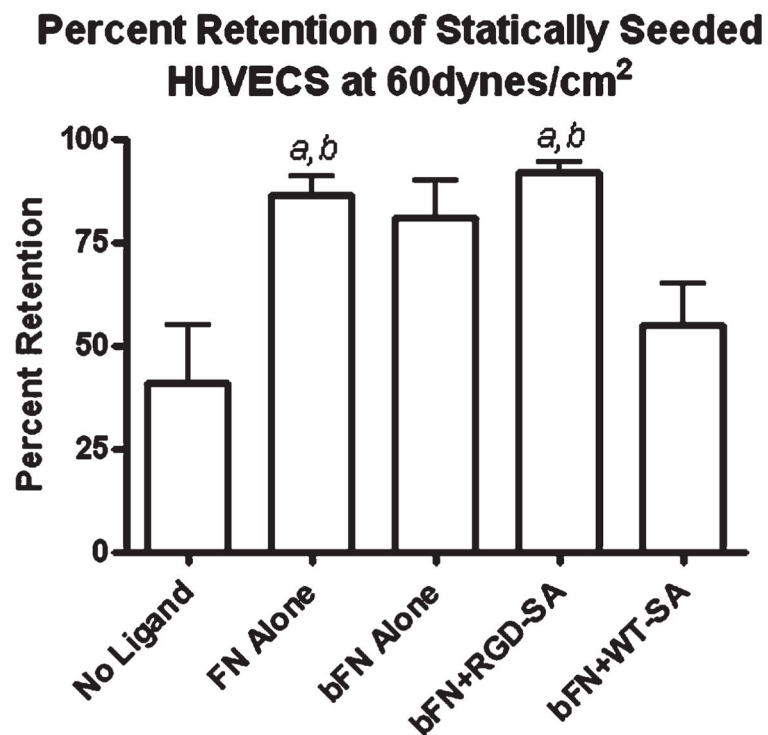


**Figure 1.** Percent retention of HUVEC statically seeded onto Teflon-AF with different ligand treatments at 60 dynes/cm<sup>2</sup>. The cells were seeded statically for 15 min prior to flow perturbation: (a) larger than no ligand and (b) larger than bFN + WT-SA. There were no statistical differences observed between FN alone, bFN alone, and bFN + RGD-SA treatment groups ( $n = 4$ ). Statistical differences ( $p < 0.05$ ).

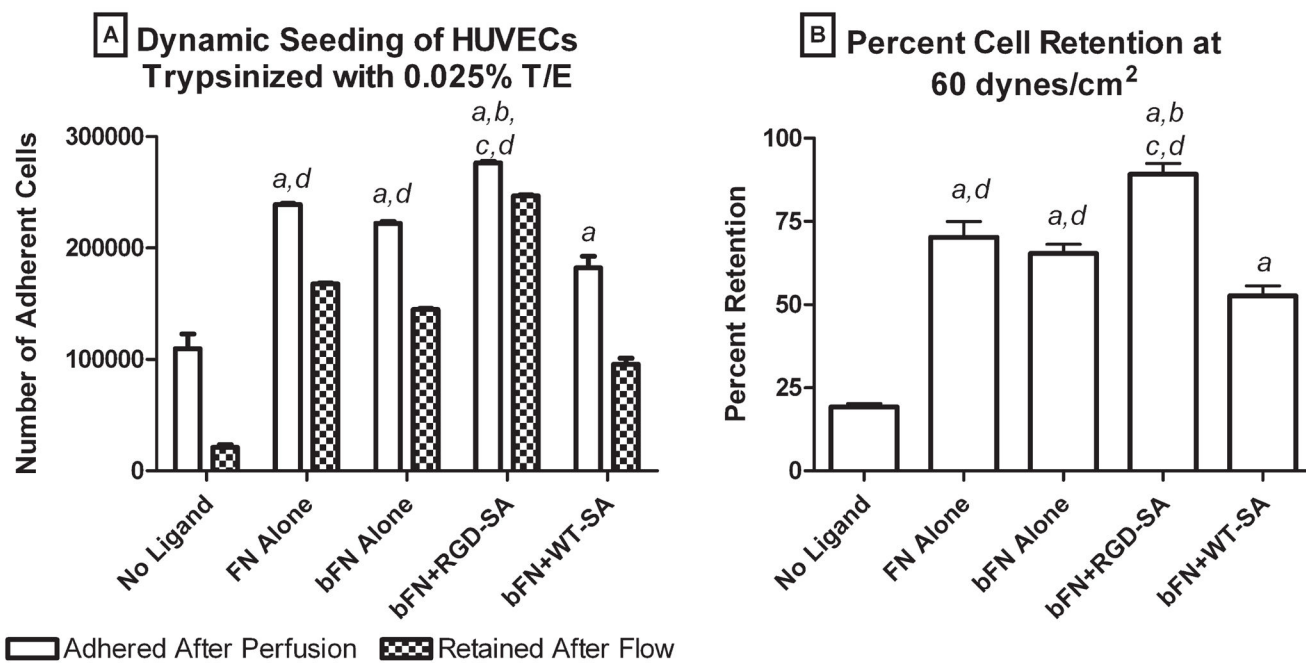


**Figure 2.** (A) Number of adherent cells and (B) cell retention for mildly trypsinized HUVECs on surfaces with no ligand, FN alone, bFN alone, bFN + RGD-SA, and bFN + WT-SA: (a) larger than no ligand, (b) larger than FN alone, (c) larger than bFN, and (d) larger than bFN + WT-SA. Error bars represent standard error of the mean ( $n = 4$ ). Statistical differences ( $p < 0.05$ ).

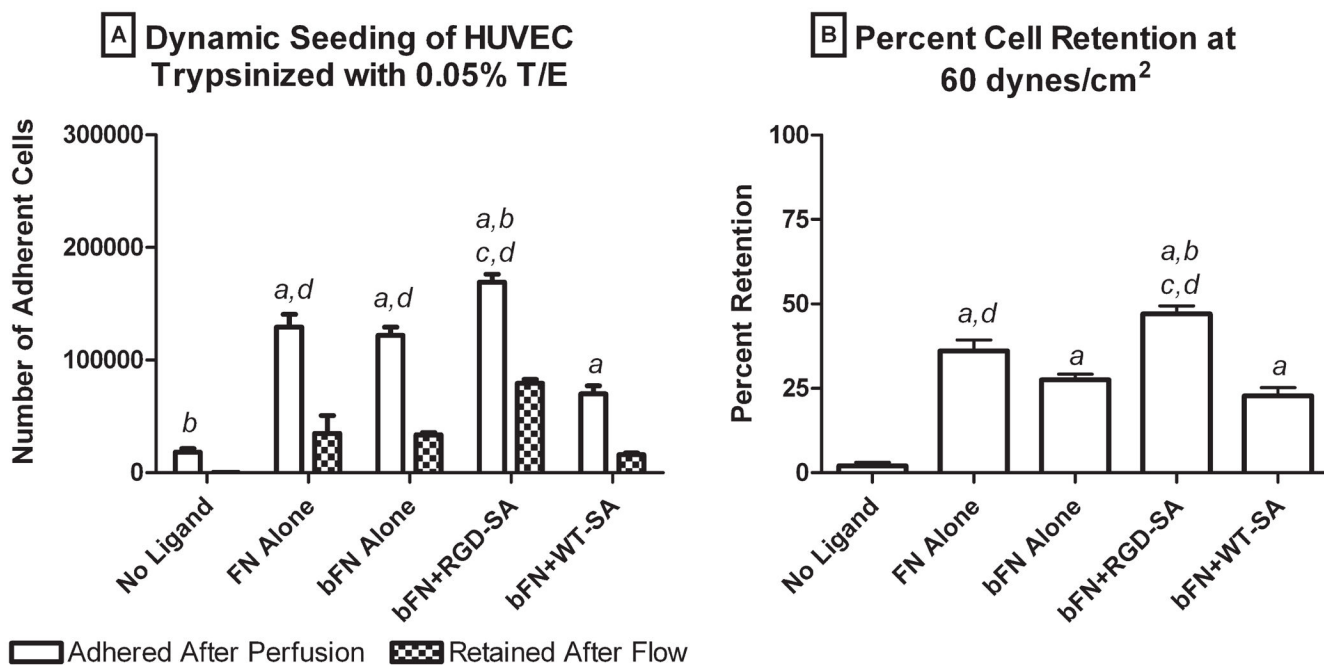


**Figure 3.** (A) Number of adherent cells and (B) cell retention for harsher trypsinized HUVECs on surfaces with no ligand, FN alone, bFN alone, bFN + RGD-SA, and bFN + WT-SA: (a) larger than no ligand, (b) larger than FN alone, (c) larger than bFN alone, and (d) larger than bFN + WT-SA. Error bars represent standard error of the mean ( $n = 4$ ). Statistical differences ( $p < 0.05$ ).

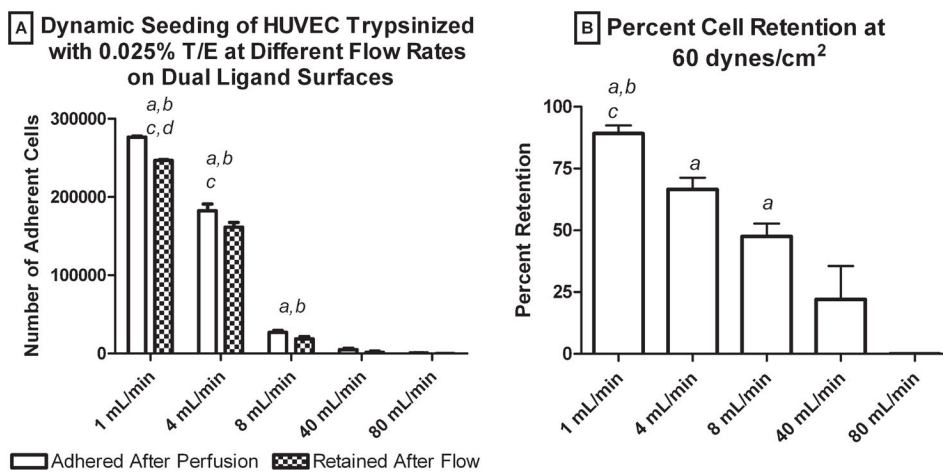


**Figure 4.** (A) Number of adherent cells and (B) cell retention for cells perfused at different flow rates on surfaces with bFN + RGD-SA: (a) larger than 80 mL/min, (b) larger than 40 mL/min, (c) larger than 8 mL/min, and (d) larger than 4 mL/min. Error bars represent standard error of the mean ( $n = 4$ ). Statistical differences ( $p < 0.05$ ).

### Integrin Binding to Immobilized Protein

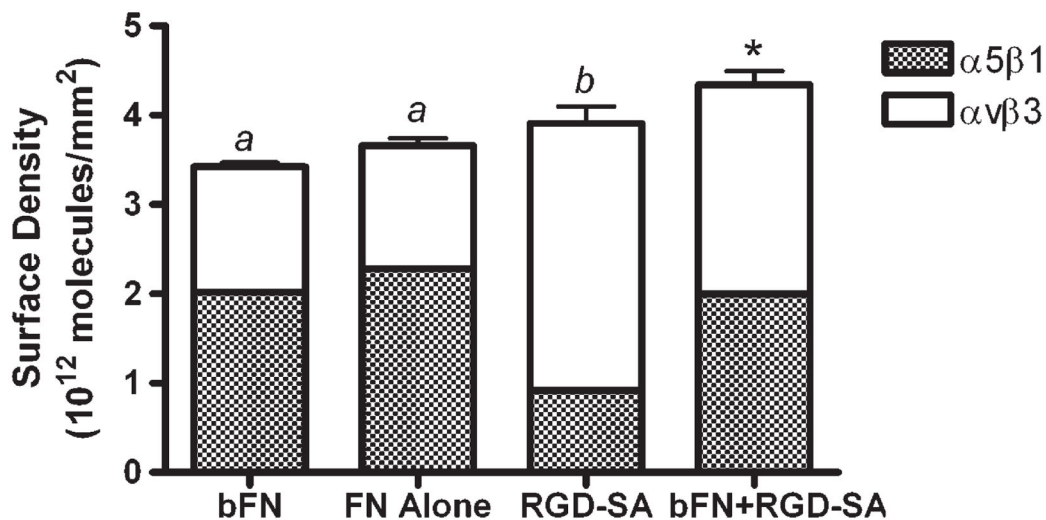


**Figure 5.**  $\alpha_5\beta_1$  and  $\alpha_V\beta_3$  integrin bound to immobilized bFN, RGD-SA, and bFN + RGD-SA: (a) larger than  $\alpha_V\beta_3$  integrin binding and (b) larger than  $\alpha_5\beta_1$  integrin binding. (\*) Statistically different from bFN and RGD-SA. Error bars represent standard error of the mean ( $n = 4$ ). Statistical differences ( $p < 0.05$ ).